

# Anomalous Criticality of Absorbing State Transition toward Jamming

He-Da Wang,<sup>1, 2, 3</sup> Bo Wang,<sup>1, 2, 3</sup> Qun-Li Lei,<sup>1, 2, 3, 4, \*</sup> and Yu-Qiang Ma<sup>1, 2, 3, 4, †</sup>

<sup>1</sup>*National Laboratory of Solid State Microstructures, Nanjing University, Nanjing 210093, China*

<sup>2</sup>*Collaborative Innovation Center of Advanced Microstructures and School of Physics, Nanjing University, Nanjing 210093, China*

<sup>3</sup>*Jiangsu Physical Science Research Center, Nanjing 210093, China*

<sup>4</sup>*Hefei National Laboratory, Shanghai 201315, China*

(Dated: October 9, 2025)

**Abstract:** The jamming transition is traditionally regarded as a geometric transition governed by static contact networks. Recently, dynamic phase transitions of athermal particles under periodic shear provide a new lens on this problem, leading to a conjecture that jamming transition corresponds to an absorbing-state transition within the Manna (conserved directed percolation) universality class. Here, by re-examining the biased random organization model, a minimal model for particles under periodic shearing that the conjecture bases on, we uncover several criticality anomalies at high density beyond the description of Manna universality class. In three-dimensional monodisperse systems, crystallization disrupts the absorbing transition, while in dense binary mixtures, a distinct transition from absorbing to active-glass states emerges, signifying a new universality class of dynamic phase transitions. Closer to jamming point, the quenched heterogeneity in the contact network smears the dynamic transition via Griffiths effects and drives the system toward heterogeneous directed percolation. We further proposal a field theory with fractional time dynamics that unifies these phenomena, establishing a theoretical framework linking jamming, disorder, and dynamic criticality.

## SIGNIFICANCE

The jamming transition, when materials like sand or foam suddenly become rigid, is traditionally viewed as a geometric packing problem. Recent ideas suggest it's also tied to a criticality of dynamic processes, like how crowded particles stop moving under repeated shaking or shearing. This work puts these ideas to the test and reveal a more complex and fascinating story: at intermediate high density, a new universality class emerges, marking a transition from absorbing to active-glass states, while near the jamming point, heterogeneity induces Griffiths effects smearing out the dynamic critical point. Our work reveals complicated interplay between static and dynamic phase transitions and sheds lights on the dynamic criticality of high-dimensional disordered systems, like learning processes of artificial neuron networks.

## INTRODUCTION

The jamming transition, a transition from a mechanically soft state to a rigid state, widely exists in soft matter systems [1–4]. The static packing of spheres provides a natural route to study the jamming transition, in which the random close packing (RCP) state is introduced to describe the most compact state that spheres can be arranged in a random way [5–7]. Although the RCP state can be protocol-dependent [8, 9], it is still widely believed to be a signature of the jamming transition [10–16].

Another path to tackle the jamming problem is from the dynamic side. It was first found that when dilute suspended colloidal particles are subjected to periodic

shearing, a reversible to irreversible transition, or an absorbing phase transition, can occur upon increasing the shearing amplitude [17–19]. As system density increases, the critical shearing amplitude becomes smaller, making the reversible to irreversible transition coincide with the jamming transition [4, 19–28]. Nevertheless, directly studying the criticality of such dynamic transition at high density is challenging, due to the diverging relaxation time and long-range correlation between particles [19, 21–23]. Theoretically, the many-body dynamics of particles under periodic shearing can be well captured by a minimal model, i.e., the random organization (RO) model [18]. Recent works have demonstrated that the biased random organization (BRO) model, a more realistic version of the RO model, can generate the RCP state at the critical point of the absorbing transition when the displacement size (corresponding to shearing amplitude) is vanishing  $\varepsilon \rightarrow 0$  in dimensions  $d=3$  to  $5$  [29–31]. The RO/BRO model in the dilute regime has been proven to belong to the Manna universality class, or conserved directed percolation [32–34]. In Ref. [29, 30, 35], it was suggested that the BRO model also resides in the Manna universality class in the close packing limit ( $\varepsilon \rightarrow 0$ ). Nevertheless, a comprehensive and detailed study of the dynamic criticality of the BRO model in the high density regime is needed to fully resolve this issue.

In this work, we show that the BRO model exhibits anomalous critical behaviors at high density, which deviates from Manna universality class. In 3D monodisperse sphere systems, we find that the absorbing transition is interrupted by crystallization. In binary mixture systems without crystallization, an unreported universality of dynamic phase transition, i.e., absorbing to active-

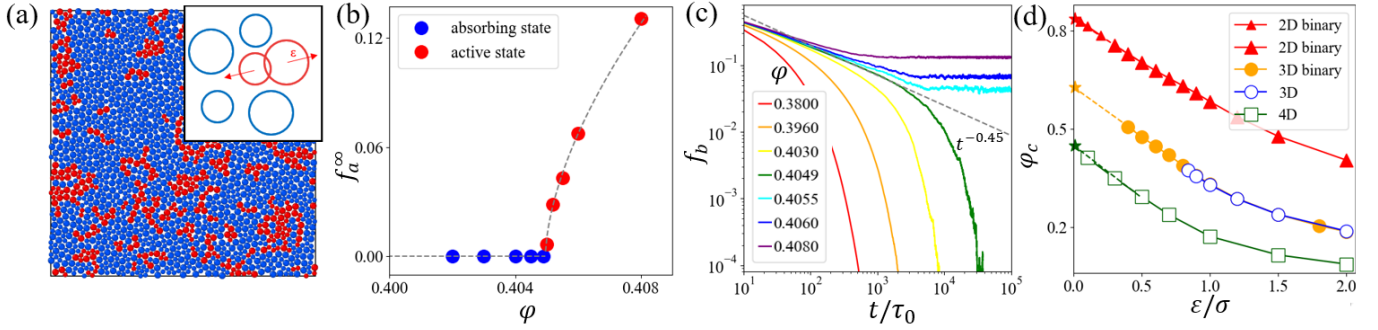


FIG. 1: (a) Schematic of the BRO model: overlapping particles (red) become active and take pairwise repulsive displacements. (b)  $f_a^\infty$  as a function of packing fraction  $\varphi$  at  $\epsilon=2.0\sigma$ . (c) Evolution of  $f_b(t)$  for systems at  $\epsilon=2.0$  under various  $\varphi$ . The dashed line represents the power law  $t^{-0.45}$ . Here  $N=65536$ . (d) Critical packing fractions  $\varphi_c$  for 2D binary (red line), 3D binary (orange dots), 3D monodisperse (blue circles) and 4D monodisperse (green open squares) systems at different  $\epsilon$ . Asterisks mark the extrapolated  $\varphi_c$  for  $\epsilon \rightarrow 0$ , i.e., 0.840 (2D) and 0.638 (3D) and 0.455 (4D), which is consistent with the RCP.

glass transition, is identified, which is characterized by critical exponents different from the Manna universality. With further increasing the critical density by decreasing  $\epsilon$ , dynamic heterogeneity and Griffiths effects emerge, which smooth the dynamic transition and broaden the critical point into a pseudo-critical regime. As  $\epsilon \rightarrow 0$ , the dynamic transition becomes equivalent to heterogeneous directed percolation (DP) due to particle immobility set by the jamming. These results indicates that while the BRO model can generate RCP configurations, the criticality of the transition is fundamentally reshaped by the RCP state. This discourages a direct mapping of the jamming transition to an absorbing phase transitions. At last, we also propose a field theory with fractional time dynamics which can describe the transition from absorbing to active-glass transition and heterogeneous DP in the same framework, revealing a complicated interplay between dynamic criticality and spatial annealed/quenched disorder. Our findings can be a starting point to study the criticality of dynamic phase transition in more complicate disordered systems, like the learning process of artificial neuron networks [31, 36].

## MODEL AND SIMULATIONS

In the BRO model, particles are first randomly distributed in the space of dimension  $d$ . In each discrete time step, if a particle is isolated without overlapping with other particles, it is considered inactive and remains stationary. On the contrary, if two particles overlap, they are considered as active and a pair of repulsive displacements with opposite direction are assigned to each other. The displacement pair has the same magnitude randomly chosen from uniform range of  $[0, \epsilon/2]$ , as shown in Fig. 1(a). If a particle overlaps multiple particles, pairwise displacements are superimposed [29–31]. We simulate  $N$  spherical particles in a square box of length  $L$  with periodic boundary conditions at packing

fraction  $\varphi$ . Both the monodisperse particle system and equal-number binary mixture of small and large particles are considered. In the latter, the particle diameter ratio is  $\sigma_M/\sigma_m=1:\sqrt{2}$  for 2D systems. For 3D systems, a larger particle diameter ratio  $\sigma_M/\sigma_m=1:1.6$  is also considered. The small particle diameter in each system is chosen as the unit length  $\sigma$ .

To study the dynamic criticality of the system, we analyze the ensemble of dynamic trials starting from random configurations. We define the survival activity of the system at time  $t$

$$f_a(\tau, t) = \frac{\langle N_a(\tau, t) \rangle_a}{N} \quad (1)$$

where  $N_a(t)$  is the number of active particles at time step  $t$ . Here,  $\tau=(\varphi-\varphi_c)/\varphi_c$  is the distance to the critical point. Note that  $\langle \rangle_a$  here indicates that the average is done only for trials that remain active up to time  $t$ . Generally, below the critical point ( $\tau < 0$ ), the system falls into an absorbing phase with  $f_a^\infty \equiv f_a(t \rightarrow \infty) = 0$ , while above the critical point ( $\tau > 0$ ), the system stays in an active state with  $f_a^\infty > 0$  (see Fig. 1(b)). At the critical point ( $\tau = 0$ ),  $f_a(t)$  is expected to decay following a power law  $t^{-\alpha}$ . We can further define the overall activity of the system averaged over all trials

$$f_b(\tau, t) = \frac{\langle N_a(t) \rangle}{N} = f_a(\tau, t) P_s(\tau, t) \quad (2)$$

where  $P_s(\tau, t)$  is the survival probability of the active phase up to time  $t$ . At the critical point,  $f_b(t)$  should also decay following a power law  $t^{-\alpha}$ . Below and above the critical point,  $f_b(t)$  deviates from the power law as shown in Fig. 1(c). As shown later,  $f_b(t)$  provides a good measure of the Griffiths effect. Details about the finite size scaling of  $f_a(\tau, t)$ ,  $f_b(\tau, t)$  and  $P_s(\tau, t)$ , the definition of critical exponents and other quantities can be found in the Methods section.

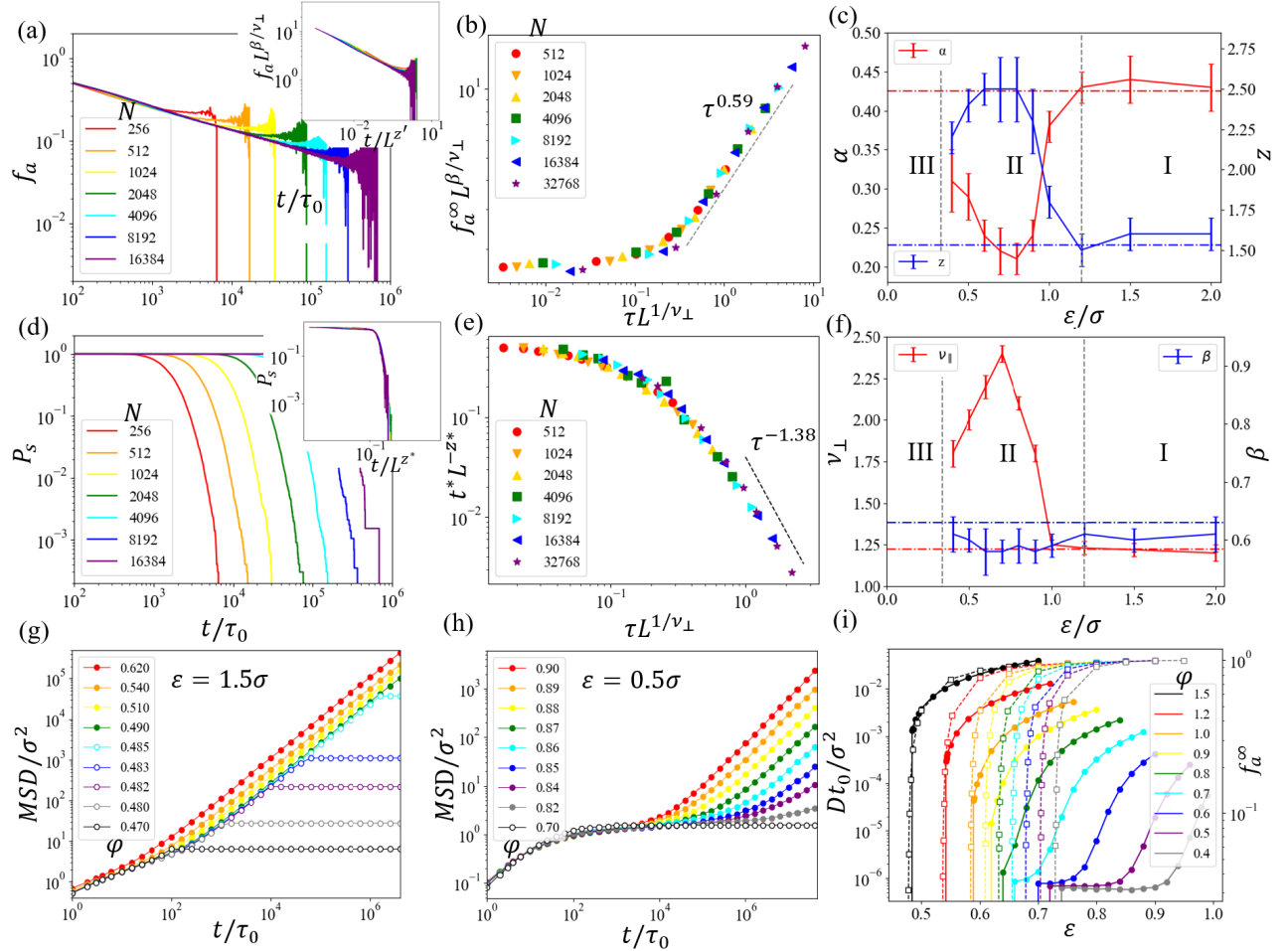


FIG. 2: (a, d) Finite size scaling for survival activity  $f_a(t)$  and survival probability  $P_s(t)$  at  $\varepsilon=0.8\sigma$ ,  $\varphi_c=0.6324$ , from which we obtain  $\alpha=0.21$ ,  $z=2.75$ . (b, e) Finite size scaling for  $f_a^\infty$  and  $t^*$  at  $\varepsilon=0.8\sigma$ . (c, f) Critical exponents of  $\beta$ ,  $\nu_\parallel$ ,  $\alpha$ ,  $z$  as functions of  $\varepsilon$ , from which one can distinguish three regimes, I, II, III. Red and blue dotted lines represent the value of  $\alpha$ ,  $z$ ,  $\nu_\parallel$ ,  $\beta$  in the Manna universality. (g, h)  $MSD(t)$  for systems with  $\varepsilon=1.5\sigma$  (g) and  $\varepsilon=0.5\sigma$  (h), where the open/solid symbols represent the absorbing/active state. (i) Diffusion coefficients  $D$  (solid line) and  $f_a^\infty$  (dotted line) as functions of  $\varphi$  at various  $\varepsilon$ .

## RESULTS

**Anomalous critical behaviors at high density**  
 Based on the finite size scaling analysis, we can determine the critical packing fraction  $\varphi_c$  of the system under different  $\varepsilon$ , which are summarized in Fig. 1(d). By extrapolating these data to  $\varepsilon \rightarrow 0$ , we obtain  $\varphi_c=0.840$  in 2D,  $\varphi_c=0.638$  in 3D,  $\varphi_c=0.455$  in 4D for both monodisperse and binary systems. This is consistent with the reported RCP packing fractions  $\varphi_{RCP}$  [7, 10–13], and in line with previous studies [29, 30].

Nevertheless, for high density 3D monodispersed systems with  $\varepsilon < 0.8\sigma$ , we find that the absorbing transition is interfered by crystallization, thus does not exhibit standard critical phenomena (see Fig. S1). Although binary systems can avoid crystallization, their critical behaviors do not match the Manna universality. In Fig. 2(a, b, d, e), we show the finite-size scaling of  $f_a(t)$ ,  $P_s(t)$ ,

$f_a^\infty(\tau)$  and  $t^*(\tau)$  for 2D binary systems with  $\varepsilon=0.8\sigma$  at  $\varphi_c=0.6324$ . This finite-size scaling is different from the typical BRO model with a large step size ( $\varepsilon=1.5\sigma$ ) (see Fig. S3). The obtained critical exponents  $\beta$ ,  $\nu_\parallel$ ,  $\alpha$ ,  $z$  as functions of  $\varepsilon$  are shown in Fig. 2(c, f), where for  $\varepsilon > 1.0\sigma$  (Regime I), these critical exponents are consistent with the Manna universality. When  $0.3\sigma < \varepsilon < 1.0\sigma$  (Regime II), we find non-monotonic behaviors in  $\nu_\perp$ ,  $\alpha$ , and  $z$  inconsistent with the Manna universality. Further decreasing  $\varepsilon$  below  $0.3\sigma$  (Regime III), the failure of standard finite size scaling and the uncertainty of the critical point are observed. It should be noted that the exponent  $\beta$  does not change significantly in Regimes I and II. The measured  $z$ ,  $z'$ , and  $z^*$  are consistent, and  $\nu_\perp=z/\nu_\parallel$  also changes with  $\varepsilon$  (see Fig. S2). In Fig. S2-6, we also present the exponents measured in the 3D system under two different particle diameter ratios, as well as the mono-dispersed 4D system. We find that the general behavior of the critical exponent and finite size scaling

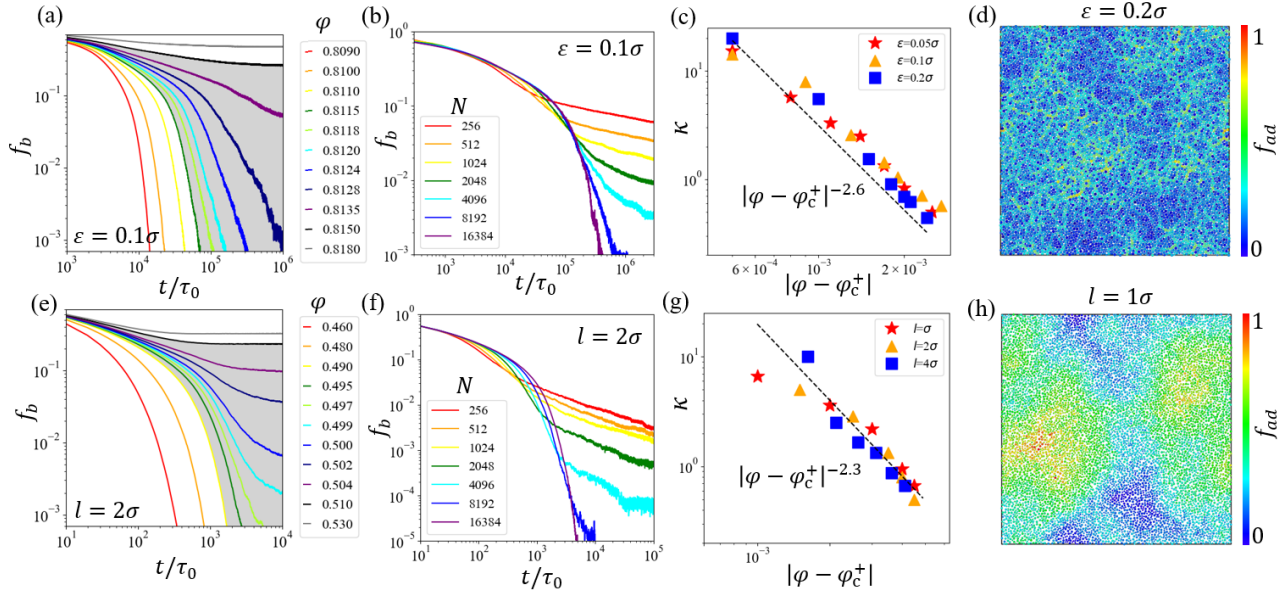


FIG. 3: (a, e) Evolution of  $f_b(t)$  at different  $\varphi$ , where Griffiths regime is painted in gray. (b, f) Evolution of  $f_b(t)$  at different  $N$ . And  $\varphi=0.8128$ (upper) and  $0.4920$  (lower). (c, g) Relationship between index  $\kappa$  and  $\varphi$ . (d, h) Distributions of normalized activity duration  $f_{ad}$  at  $\varphi=0.7838, \varepsilon=0.2\sigma$ (upper) and  $0.4980, \varepsilon=1.5\sigma, \Delta\epsilon=1.2\sigma, l=1\sigma$  (lower). (a, b) are for the original BRO model with  $\varepsilon=0.1\sigma$ . (e, f) are for modified BRO models with quenched-disorder at  $\varepsilon=1.5\sigma, \Delta\epsilon=1.2\sigma$  and  $l=2\sigma$ . For all systems except (b,f),  $N=8192$ .

remain unchanged. This indicates that the anomalous criticality of the BRO model are robust at high density, insensitive to the dimensionality and particle diameter ratio.

**Absorbing to active-glass transition** We first focus on the Regime I where the step size  $\varepsilon$  is larger than the particle size. In this regime, the motion of active particles is not constrained by neighbouring particles. Thus, the mean-square-displacement (MSD) of active particles shows diffusion scaling as shown in Fig. 2(g). Here, the solid and open symbols represent systems above and below the critical point, respectively. The diffusion scaling in sub-critical systems indicates that the absorbing transition is essentially a non-local searching process for a non-overlapping configurations, consistent with Manna (CDP) universality [37, 38].

As  $\varepsilon$  decreases,  $\varphi_c$  increases. Due to the repulsive displacement in the BRO model, the particles are caged by their neighbours. This effect is shown in Fig. 2(h) for systems with  $\varepsilon=0.5\sigma$ , where one can find a early-time plateau or sub-diffusion regime in MSD for system near the critical point, a characteristic of the glass-forming liquids [39–42]. In Fig. 2(i), we plot the measured diffusion coefficient  $D$  of active particle and  $f_a^\infty$  as a function of  $\varphi$  under different  $\varepsilon$ . We can clearly distinguish active states with  $D$  as low as  $10^{-6}\sigma^2/\tau_0$  for  $\varepsilon \lesssim \sigma$ . The decoupling between  $f_a^\infty$  and  $D$  suggests that in this regime (Regime II), the absorbing phase transition is essentially an absorbing to active-glass transition, where particles can only find a non-overlapping absorbing configuration

through local arrangements instead of non-local searching.

The fundamental difference between these two scenarios can be distinguished by field theory. For Manna (CDP) universality, it can be described by an non-conserved field  $\rho(\mathbf{r}, t)$  (active particle density field) coupling with a non-diffusive conserved field  $\psi(\mathbf{r}, t)$  (total density field)[43, 44], namely,

$$\frac{\partial \rho(t)}{\partial t} = D \nabla^2 \rho + a \rho - b \rho^2 + \omega \rho \psi + \sigma_n \sqrt{\rho} \xi(t) \quad (3)$$

$$\frac{\partial^\theta \psi(t)}{\partial t^\theta} = D' \nabla^2 \rho, \quad (4)$$

with  $\theta=1$  indicating the evolution of  $\psi(t)$  field is a result of diffusion of  $\rho(t)$  field. Note that  $a, b, w$  are fixed parameters determining the critical point[44]. The last term in Eq.(4) is the multiplicative noise term accounting for absorbing phase transition. In the active-glass state, however, the dynamic of  $\psi(t)$  field in Eq.(4) is sub-diffusive, corresponding to fractional time derivative with  $0 < \theta < 1$ [45, 46]. Obviously, the criticality with fractional time dynamics distinguish itself from Manna universality. The observed continuous variation of critical exponents in this regime might be due to the variation of  $\theta$ . Nevertheless, numerical solution and renormalization-group analysis of this fractional time equation with multiplicative noise is currently challenging [45, 46].

**Griffiths effect in pre-jamming state** When  $\varepsilon$  is further reduced below  $0.3\sigma$  (Regime III), the critical density of the system would approach to that of RCP state.

In this regime, caging-breaking events becomes unlikely and the topology of particle network remains unchanged in the activation process. We refer this state as the pre-jamming state. Different from the conventional absorbing phase transition, we find  $f_b(t)$  in this state relaxes according to a continuous power law

$$f_b(t) \sim t^{-d/\kappa} \quad (5)$$

with the  $\varphi$ -dependent critical exponent

$$\kappa \sim |\varphi - \varphi_c^+|^{-h} \quad (6)$$

in a wide density range  $\varphi_c^- < \varphi < \varphi_c^+$ , as shown in Fig. 3(a) and Fig. S7. Here  $h$  is the exponent for the ‘dirty’ critical point  $\varphi_c^+$  [47]. The existence of this critical-like regime rather than critical point, is a strong evidence of the Griffiths effect which is usually caused by spatial heterogeneity [47–52]. These effect becomes more pronounced with decreasing  $\varepsilon$  as shown in Fig. S7. In Fig. 3(c), we plot the measured  $\kappa$  as function of  $|\varphi - \varphi_c^+|$ , which gives  $h=2.6$ .

In the Griffiths phase, the quenched disorder generates strong dynamic heterogeneity in the relaxation process. This can be visualized by the spatial distribution of normalized activity duration  $f_{ad}$ , i.e., the fraction of time that a particle stays in an active state relative to the active duration of the whole system, starting from a perturbed absorbing configuration. In Fig. 3(d), we show these distributions for systems with  $\varepsilon=0.2\sigma$ . One can observe non-uniform network structures of activity, resembling the dynamic heterogeneity of a supercooled liquids or the force chain of the jammed state [53–55]. In Regime II, one can also find relative weak dynamic heterogeneity (Fig. S9), which would be smoothed out by further increasing  $\varepsilon$  to Regime I.

In the Griffiths phase, the finite-size effect of  $f_b(t)$  and  $P_s(t)$  near criticality are also reversed, i.e., at the same density near the transition, small systems stay longer in the active state than large systems. This is best shown in Fig. 3(b) and Fig. 4(a), as well as in Fig. S3. This abnormality is nevertheless consistent with the fact that small systems are more likely be jammed near the jamming point [56, 57]. This suggests that close-packing significantly influences the criticality of absorbing phase transition in this regime. Further support comes from the structure factor  $S(q)$  for systems with  $\epsilon \rightarrow 0$ , which does not follow the  $q^{0.45}$  scaling of the Manna model (see Fig. S8).

To further prove that the above phenomena are results of Griffiths effect, we manually add quenched disorder in systems located at Regime I, by making  $\varepsilon$  spatially dependent. More explicitly, the system is divided into cells of size  $l$ . Each cell  $(i,j)$  has its own  $\varepsilon_{i,j}$  set as

$$\tilde{\varepsilon}_{i,j} = \varepsilon + \Delta\varepsilon \xi_{i,j} \quad (7)$$

where  $\Delta\varepsilon$  is the strength of the quenched disorder and  $\xi_{i,j}$  is a spatially-uncorrelated random number uniformly

distributed within  $(-1, 1)$ . Thus for  $\Delta\varepsilon=0$ , we return to the original BRO model. In Fig. 3(e, f), we show  $f_b(t)$  and the activity duration distribution for systems under  $\varepsilon=1.5\sigma$  and  $\Delta\varepsilon=1.2\sigma$ . Compared with  $\Delta\varepsilon=0$  cases that exhibits standard critical behaviors, introduction of  $\Delta\varepsilon$  induces obvious dynamic heterogeneity and the Griffiths effect similar to Fig. 3(a, b). In Fig. 3(f, g), we plot the finite-size scaling of  $f_b(t)$  and  $\kappa(|\varphi - \varphi_c^+|)$  for these systems, which exhibits strong similarity with high density systems shown Fig. 3(b, c). Moreover, we find that the effect of increasing  $l$  (correlation length of quenched disorder), is similar to decreasing  $\varepsilon$  in pre-jamming states (Fig. S7). This indicates that the correlation length diverges in BRO model as  $\varepsilon \rightarrow 0$ , in accordance with what happens at the jamming transition point [58].

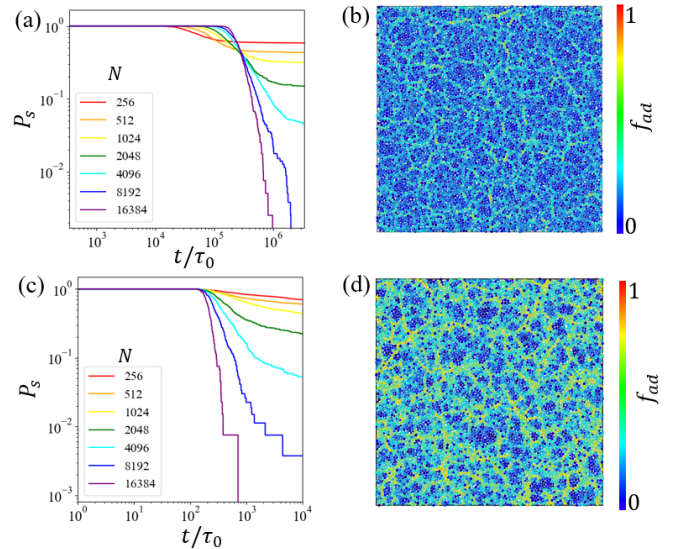


FIG. 4: (a, c) Finite size effects of survival probability of dynamic trajectory  $P_s(t)$ . (b, d) Distributions of normalized activity duration. (a, b) are for the original BRO models near the transition point at  $\varepsilon=0.05\sigma$  and  $\varphi=0.8380$ . (c, d) are for the heterogeneous contact model at  $P_e=0.795$  and  $k=1$  based on the same configuration as in (b).

**Mapping to heterogeneous DP** Finally, we study the critical behaviors of the BRO model in the close packing limit ( $\varepsilon \rightarrow 0$ ). In this limit, the particle configuration can be regarded as static during the relaxation process. From the point of field theory, this scenario corresponds to  $\theta=0$  in Eq.(4), where the evolution of density field  $\psi$  is completely forbidden. Thus, the density field  $\psi$  acts as pure quenched disorder in the dynamics of  $\rho$  field, essentially changing the CDP universality to the directed percolation (DP) universality [47, 49, 50]. The classical contact model is the simplest realization of DP [59, 60]. To test this idea, we simulate a contact model on the networks composed of nearly jammed particles generated by the BRO model at  $\varepsilon=0.05\sigma$ , where each particle represents a node. We find that the topology of the contact

network alone does not affect the critical behaviours of systems. However, if the infection rate of a node is proportional to the activity durations of the corresponding particle (see the Method section for details), the activity distribution of this contact model exhibits dynamic heterogeneity resembling that of the high density BRO model, as shown in Fig. 4(b, d). Correspondingly, the finite size scaling of  $P_s(t)$  in Fig. 4(c) also exhibits similar anomalous behaviors as the BRO model in the close packing limit Fig. 4(a). This similarity proves that the critical behaviors of the BRO model in the nearly jammed configuration corresponds to DP on hierachic heterogeneous network. Moreover, the Griffith effect becomes stronger as the heterogeneity increases in DP model (see Fig. S11). It should be noted that our previous modified BRO model with cell-size quenched-disorder fails to account Griffith effect at the closed packing limit, because the correlation in this point span the system size, leaving the topology of heterogeneous network play the dominant role.

## CONCLUSION

In summary, we investigate the critical behavior of the BRO model in dense monodisperse and binary systems in  $d=2$  to 4. We find that anomalous critical phenomena emerge as the critical density increases by decreasing  $\varepsilon$ . For 3D monodispersed systems at intermediate critical density, the crystallization interrupts the dynamic phase transition. For binary systems at intermediate critical density, the measured critical exponents deviate from the Manna universality class due to the caging effects, signifying the existence of new universality of dynamic phase transition, i.e., an absorbing to active glass transition. For both monodispersed and binary systems at higher density, the quenched disorder of contact networks triggers pronounced Griffiths effect, smearing out the dynamic phase transition. In the  $\varepsilon \rightarrow 0$  limit, the BRO model becomes equivalent to DP on heterogeneous network. Our results demonstrate that although the BRO model can generate RCP configurations, the criticality of the dynamic transition is fundamentally reshaped by the geometric rigidity of the RCP state. These findings discourage previous attempts to directly associate the jamming transition with the Manna universality class. We also propose a field theory with fractional time dynamics which unifies both the absorbing to active-glass transition and heterogeneous DP, revealing a deep connection between dynamic criticality and spatial annealed/quenched disorder. Our work could potentially be related to ultra-stable glass and the Gardner transition [61–64] and open a door to study the dynamic criticality of more complicated artificial neuron networks [36], like the learning process of spherical negative perceptron model [31].

## METHOD

**Finite-size scaling of absorbing phase transition** For typical second-order absorbing phase transitions,  $f_a(t)$  should satisfy the finite-size scaling relationship [65–67]

$$f_a(t, \tau, L) \propto L^{-\beta/\nu_{\perp}} \mathcal{F}(tL^{-z'}, \tau L^{1/\nu_{\perp}}) \quad (8)$$

where  $\mathcal{F}(x, y)$  is the scaling function satisfying  $\mathcal{F}(x, 0) \sim x^{-\alpha}$  for  $x \ll 1$  and  $\mathcal{F}(x, 0) \sim \text{const.}$  for  $x \gg 1$ . In a fully active state, the decay of  $f_a(t, 0, L)$  is independent of  $L$  at an earlier stage, which leads to  $z' = \beta/(\nu_{\perp} \alpha)$ . On the other hand,  $f_a^\infty$  satisfies

$$f_a^\infty(\tau, L) \propto L^{-\beta/\nu_{\perp}} \mathcal{F}(\infty, \tau L^{1/\nu_{\perp}}) \quad (9)$$

where  $\mathcal{F}(\infty, y) \sim y^\beta$  for  $y \gg 1$  and  $\mathcal{F}(\infty, y) \sim \text{const.}$  for  $y \ll 1$ . Furthermore, the survival probability  $P_s(\tau, t)$  of the active phase up to time  $t$  should satisfy

$$P_s(t, \tau, L) \propto \mathcal{P}(tL^{-z^*}, \tau L^{1/\nu_{\perp}}) \quad (10)$$

where  $\mathcal{P}(x, 0) \sim 1$  for  $x \ll 1$  and  $\mathcal{P}(x, 0) \rightarrow 0$  for  $x \gg 1$ . From Eq. (10), we can also obtain the finite size scaling relationship for the characteristic time of the active spreading process  $t^*$  satisfying  $\mathcal{P}(t^* L^{-z^*}, \tau L^{1/\nu_{\perp}}) = 0.5$ , i.e.,

$$t^* \propto L^{z^*} \mathcal{T}(\tau L^{1/\nu_{\perp}}) \quad (11)$$

where  $\mathcal{T}(x) \sim \text{const.}$  for  $x \ll 1$  and  $\mathcal{T}(x) \rightarrow x^{-\nu_{\parallel}}$  for  $x \gg 1$ . By definition,  $z = \nu_{\parallel}/\nu_{\perp}$  is the dynamic critical exponent. For a typical absorbing phase transition, one should expect  $z = z' = z^*$ .

**Heterogeneous contact model** In the classical contact model, two important controlling parameters are the basic infection rate  $P_e$  and recovery rate  $P_r$ . The probability that the healthy site  $i$  becomes infected by an adjacent infected site in the next time step is

$$P_{e,i} = P_e \frac{n_a(i)}{n_{neib}(i)} \quad (12)$$

where  $n_a(i)$  represents the number of infected neighbors of the particle  $i$ , and  $n_{neib}(i)$  is the total number of neighbors of the particle  $i$ . The recovery rate of each site, i.e., the probability that an infected site becomes healthy in the next time step, is  $P_r = 1 - P_e$ . We establish a contact network based on the particle configuration generated by BRO dynamics, where the positions of particles are the nodes of the network. A contact bond is assumed between the two nodes if their distance is less than  $0.5\sigma$ . We introduce the heterogeneity by making the infection rate of site  $i$  undermined by the activity duration  $f_{ad}(i)$  of the particle, i.e.,

$$P_{e,i} = f_{ad}(i)^k P_e \frac{n_a(i)}{n_{neib}(i)}. \quad (13)$$

Here  $f_{ad}(i)$  is in the range of  $(0, 1)$ . As  $k$  increases, the heterogeneity becomes more prominent. We calculated the data of changing the basic infection rate  $P_e$  when  $k=1, 2$  and  $4$ . We find that the Griffith effect become stronger as  $k$  increases (see Fig. S11).

**Acknowledgments:** The authors are grateful to Ran Ni, Ning Xu, Hao Hu and Hua Tong for helpful discussion. This work is supported by the National Natural Science Foundation of China (No. 12347102, No. 12275127), the Innovation Program for Quantum Science and Technology (No. 2024ZD0300101), the Natural Science Foundation of Jiangsu Province (No. BK20250058, No. BK20233001), Program for Innovative Talents and Entrepreneur in Jiangsu, the Fundamental Research Funds for the Central Universities (0204-14380249, KG202501). The simulations are performed on the High-Performance Computing Center of Collaborative Innovation Center of Advanced Microstructures, the High-Performance Computing Center (HPCC) of Nanjing University.

---

\* lql@nju.edu.cn

† myqiang@nju.edu.cn

- [1] V. Trappe, V. Prasad, L. Cipelletti, P. Segre, and D. A. Weitz, Jamming phase diagram for attractive particles, *Nature* **411**, 772 (2001).
- [2] A. J. Liu and S. R. Nagel, The jamming transition and the marginally jammed solid, *Annu. Rev. Condens. Matter Phys.* **1**, 347 (2010).
- [3] R. P. Behringer and B. Chakraborty, The physics of jamming for granular materials: a review, *Reports on Progress in Physics* **82**, 012601 (2018).
- [4] Y. Deng, D. Pan, and Y. Jin, Jamming is a first-order transition with quenched disorder in amorphous materials sheared by cyclic quasistatic deformations, *Nature Communications* **15**, 7072 (2024).
- [5] J. D. Bernal and J. Mason, Packing of spheres: coordination of randomly packed spheres, *Nature* **188**, 910 (1960).
- [6] G. D. Scott, Packing of spheres: packing of equal spheres, *Nature* **188**, 908 (1960).
- [7] J. G. Berryman, Random close packing of hard spheres and disks, *Phys. Rev. A* **27**, 1053 (1983).
- [8] S. Torquato, T. M. Truskett, and P. G. Debenedetti, Is random close packing of spheres well defined?, *Phys. Rev. Lett.* **84**, 2064 (2000).
- [9] T. Aste, M. Saadatfar, and T. J. Senden, Geometrical structure of disordered sphere packings, *Phys. Rev. E* **71**, 061302 (2005).
- [10] M. Danisch, Y. Jin, and H. A. Makse, Model of random packings of different size balls, *Phys. Rev. E* **81**, 051303 (2010).
- [11] C. Anzivino, M. Casiulis, T. Zhang, A. S. Moussa, S. Martiniani, and A. Zaccone, Estimating random close packing in polydisperse and bidisperse hard spheres via an equilibrium model of crowding, *The Journal of Chemical Physics* **158**, 044901 (2023).
- [12] L. E. Silbert, D. Ertas, G. S. Grest, T. C. Halsey, and D. Levine, Geometry of frictionless and frictional sphere packings, *Phys. Rev. E* **65**, 031304 (2002).
- [13] M. Skoge, A. Donev, F. H. Stillinger, and S. Torquato, Packing hyperspheres in high-dimensional euclidean spaces, *Phys. Rev. E* **74**, 041127 (2006).
- [14] A. Donev, S. Torquato, F. H. Stillinger, and R. Connelly, Jamming in hard sphere and disk packings, *Journal of Applied Physics* **95**, 989 (2004).
- [15] A. Donev, F. H. Stillinger, and S. Torquato, Unexpected density fluctuations in jammed disordered sphere packings, *Phys. Rev. Lett.* **95**, 090604 (2005).
- [16] D. Hexner, A. J. Liu, and S. R. Nagel, Two diverging length scales in the structure of jammed packings, *Phys. Rev. Lett.* **121**, 115501 (2018).
- [17] D. J. Pine, J. P. Gollub, J. F. Brady, and A. M. Leshansky, Chaos and threshold for irreversibility in sheared suspensions, *Nature* **438**, 997 (2005).
- [18] L. Corte, P. M. Chaikin, J. P. Gollub, and D. J. Pine, Random organization in periodically driven systems, *Nature Physics* **4**, 420 (2008).
- [19] C. Reichhardt, I. Regev, K. Dahmen, S. Okuma, and C. J. O. Reichhardt, Reversible to irreversible transitions in periodic driven many-body systems and future directions for classical and quantum systems, *Physical Review Research* **5**, 021001 (2023).
- [20] C. F. Schreck, R. S. Hoy, M. D. Shattuck, and C. S. O'Hern, Particle-scale reversibility in athermal particulate media below jamming, *Phys. Rev. E* **88**, 052205 (2013).
- [21] K. Hima Nagamanasa, S. Gokhale, A. Sood, and R. Ganapathy, Experimental signatures of a nonequilibrium phase transition governing the yielding of a soft glass, *Physical Review E* **89**, 062308 (2014).
- [22] I. Regev, T. Lookman, and C. Reichhardt, Onset of irreversibility and chaos in amorphous solids under periodic shear, *Phys. Rev. E* **88**, 062401 (2013).
- [23] I. Regev, J. Weber, C. Reichhardt, K. A. Dahmen, and T. Lookman, Reversibility and criticality in amorphous solids, *Nature communications* **6**, 8805 (2015).
- [24] T. Kawasaki and L. Berthier, Macroscopic yielding in jammed solids is accompanied by a nonequilibrium first-order transition in particle trajectories, *Phys. Rev. E* **94**, 022615 (2016).
- [25] K. Nagasawa, K. Miyazaki, and T. Kawasaki, Classification of the reversible–irreversible transitions in particle trajectories across the jamming transition point, *Soft matter* **15**, 7557 (2019).
- [26] D. Pan, Y. Wang, H. Yoshino, J. Zhang, and Y. Jin, A review on shear jamming, *Physics reports* **1038**, 1 (2023).
- [27] A. Ghosh, J. Radhakrishnan, P. M. Chaikin, D. Levine, and S. Ghosh, Coupled dynamical phase transitions in driven disk packings, *Physical Review Letters* **129**, 188002 (2022).
- [28] P. Das, H. Vinutha, and S. Sastry, Unified phase diagram of reversible–irreversible, jamming, and yielding transitions in cyclically sheared soft-sphere packings, *Proceedings of the National Academy of Sciences* **117**, 10203 (2020).
- [29] S. Wilken, R. E. Guerra, D. Levine, and P. M. Chaikin, Random close packing as a dynamical phase transition, *Phys. Rev. Lett.* **127**, 038002 (2021).

[30] S. Wilken, A. Z. Guo, D. Levine, and P. M. Chaikin, Dynamical approach to the jamming problem, *Phys. Rev. Lett.* **131**, 238202 (2023).

[31] G. Zhang and S. Martiniani, Absorbing state dynamics of stochastic gradient descent, *arXiv preprint arXiv:2411.11834* (2024).

[32] G. I. Menon and S. Ramaswamy, Universality class of the reversible-irreversible transition in sheared suspensions, *Phys. Rev. E* **79**, 061108 (2009).

[33] S. Torquato, Hyperuniform states of matter, *Physics Reports* **745**, 1 (2018).

[34] Q.-L. Lei and R. Ni, Hydrodynamics of random-organizing hyperuniform fluids, *Proceedings of the National Academy of Sciences* **116**, 22983 (2019).

[35] C. Ness and M. E. Cates, Absorbing-state transitions in granular materials close to jamming, *Phys. Rev. Lett.* **124**, 088004 (2020).

[36] S. Spigler, M. Geiger, S. d'Ascoli, L. Sagun, G. Biroli, and M. Wyart, A jamming transition from under-to over-parametrization affects loss landscape and generalization, *arXiv preprint arXiv:1810.09665 10.48550/arXiv.1810.09665* (2018).

[37] S. S. Manna, Two-state model of self-organized criticality, *Journal of Physics A: Mathematical and General* **24**, L363 (1991).

[38] K. J. Wiese, Hyperuniformity in the manna model, conserved directed percolation and depinning, *Phys. Rev. Lett.* **133**, 067103 (2024).

[39] P. G. Debenedetti and F. H. Stillinger, Supercooled liquids and the glass transition, *Nature* **410**, 259 (2001).

[40] L. Berthier and G. Biroli, Theoretical perspective on the glass transition and amorphous materials, *Rev. Mod. Phys.* **83**, 587 (2011).

[41] H. Tanaka, Structural origin of dynamic heterogeneity in supercooled liquids, *The Journal of Physical Chemistry B* **129**, 789 (2025).

[42] H. Tanaka, T. Kawasaki, H. Shintani, and K. Watanabe, Critical-like behaviour of glass-forming liquids, *Nature materials* **9**, 324 (2010).

[43] M. Rossi, R. Pastor-Satorras, and A. Vespignani, Universality class of absorbing phase transitions with a conserved field, *Physical review letters* **85**, 1803 (2000).

[44] R. Pastor-Satorras and A. Vespignani, Field theory of absorbing phase transitions with a nondiffusive conserved field, *Physical Review E* **62**, R5875 (2000).

[45] R. Metzler and J. Klafter, The random walk's guide to anomalous diffusion: a fractional dynamics approach, *Physics reports* **339**, 1 (2000).

[46] R. Metzler, E. Barkai, and J. Klafter, Anomalous diffusion and relaxation close to thermal equilibrium: A fractional fokker-planck equation approach, *Physical review letters* **82**, 3563 (1999).

[47] T. Vojta and M. Dickison, Critical behavior and griffiths effects in the disordered contact process, *Phys. Rev. E* **72**, 036126 (2005).

[48] M. A. Muñoz, R. Juhász, C. Castellano, and G. Ódor, Griffiths phases on complex networks, *Phys. Rev. Lett.* **105**, 128701 (2010).

[49] A. G. Moreira and R. Dickman, Critical dynamics of the contact process with quenched disorder, *Phys. Rev. E* **54**, R3090 (1996).

[50] J. Hooyberghs, F. Iglói, and C. Vanderzande, Absorbing state phase transitions with quenched disorder, *Phys. Rev. E* **69**, 066140 (2004).

[51] T. Vojta and M. Y. Lee, Nonequilibrium phase transition on a randomly diluted lattice, *Phys. Rev. Lett.* **96**, 035701 (2006).

[52] R. Juhász, G. Ódor, C. Castellano, and M. A. Muñoz, Rare-region effects in the contact process on networks, *Phys. Rev. E* **85**, 066125 (2012).

[53] J. F. Peters, M. Muthuswamy, J. Wibowo, and A. Tordeillas, Characterization of force chains in granular material, *Phys. Rev. E* **72**, 041307 (2005).

[54] F. Radjai, M. Jean, J.-J. Moreau, and S. Roux, Force distributions in dense two-dimensional granular systems, *Phys. Rev. Lett.* **77**, 274 (1996).

[55] T. S. Majmudar, M. Sperl, S. Luding, and R. P. Behringer, Jamming transition in granular systems, *Phys. Rev. Lett.* **98**, 058001 (2007).

[56] C. P. Goodrich, A. J. Liu, and S. R. Nagel, Finite-size scaling at the jamming transition, *Phys. Rev. Lett.* **109**, 095704 (2012).

[57] N. Xu, J. Blawzdziewicz, and C. S. O'Hern, Random close packing revisited: Ways to pack frictionless disks, *Phys. Rev. E* **71**, 061306 (2005).

[58] A. J. Liu and S. R. Nagel, Jamming is not just cool any more, *Nature* **396**, 21 (1998).

[59] T. E. Harris, Contact Interactions on a Lattice, *The Annals of Probability* **2**, 969 (1974).

[60] I. Jensen, Critical behavior of the three-dimensional contact process, *Phys. Rev. A* **45**, R563 (1992).

[61] Y. Wang, Z. Qian, H. Tong, and H. Tanaka, Hyperuniform disordered solids with crystal-like stability, *Nature Communications* **16**, 1398 (2025).

[62] L. Berthier, P. Charbonneau, Y. Jin, G. Parisi, B. Seoane, and F. Zamponi, Growing timescales and lengthscales characterizing vibrations of amorphous solids, *Proceedings of the National Academy of Sciences* **113**, 8397 (2016).

[63] P. Charbonneau, Y. Jin, G. Parisi, C. Rainone, B. Seoane, and F. Zamponi, Numerical detection of the gardner transition in a mean-field glass former, *Phys. Rev. E* **92**, 012316 (2015).

[64] Q. Wang, D. Pan, and Y. Jin, Gardner transition coincides with the emergence of jamming scalings in hard spheres and disks, *arXiv preprint arXiv:2410.23797* (2024).

[65] S. Lübeck and P. Heger, Universal finite-size scaling behavior and universal dynamical scaling behavior of absorbing phase transitions with a conserved field, *Physical Review E* **68**, 056102 (2003).

[66] B. Zheng, Generalized dynamic scaling for critical relaxations, *Phys. Rev. Lett.* **77**, 679 (1996).

[67] Q.-L. Lei, H. Hu, and R. Ni, Barrier-controlled nonequilibrium criticality in reactive particle systems, *Physical Review E* **103**, 052607 (2021).